Stamatescu, Laurentiu; Hamilton, Murray Wayne
Transfer function approach to collective mode dynamics in a Nd:YAG laser Physical Review E, 1997; 55(3):R2115-R2118

http://link.aps.org/doi/10.1103/PhysRevE.55.R2115

Transfer function approach to collective mode dynamics in a Nd:YAG laser

L. Stamatescu* and M. W. Hamilton†
Department of Physics and Mathematical Physics, University of Adelaide, Adelaide SA 5005, Australia
(Received 6 November 1996)

For a multimode laser operating in a steady state regime with small-signal gain modulation, transfer functions are measured for both total intensity and intensities of individual modes. A quantitative picture of the phase clustering of contributions from each cavity mode to the collective mode dynamics is obtained from the transfer functions in the pole-residue representation. [S1063-651X(97)50503-4]

PACS number(s): 42.65.Sf, 42.30.Lr, 42.60.Rn

Arrays of nonlinear oscillators, such as multimode lasers [1], Josephson junction arrays [2], or phase oscillators [3], can show a variety of phase locking phenomena. One is antiphase dynamics where the phases of the oscillators are clustered in one of several identified patterns [4,5] so that interference destroys the response at all but one of the coupled system eigenfrequencies. The multimode laser is particularly convenient for studying these collective modes of oscillation. Apart from the normal optical operation, each laser cavity mode shows a nonlinear relaxation oscillation at lower frequencies that corresponds to an interchange of energy between the laser medium and the optical cavity [6]. If several cavity modes are excited they can be coupled, typically through the position dependent gain sharing that is caused by the standing wave nature of the electromagnetic field for a Fabry-Pérot resonator [7] or through the inclusion of a nonlinear crystal for frequency doubling in the cavity [1].

Direct experimental confirmation of the phase clustering has been found for a three-mode laser in a limit cycle regime (spiking) [8]. For a laser in steady state operation, noise, either intrinsic or deliberately introduced, has been exploited to excite the various collective modes. In the intensity noise power spectrum for the individual laser cavity modes, one sees peaks corresponding to collective modes that are absent in the spectrum for the total intensity [9]. The latter spectrum typically shows just one remaining resonance which is the relaxation oscillation of the laser and has the highest frequency of the collective modes. However, the measurement of power spectra discards phase information, and the clustering cannot be verified directly in this technique.

We take a different approach, exciting the collective modes with a sinusoidal modulation of the laser pumping rate and measuring the response of the laser at the excitation frequency for both the total laser intensity and the individual laser modes. This is the transfer function method, which is well known in engineering and has been advocated and used [10] for theoretical analysis of this problem. The magnitude of the transfer function has also been measured [11], but, as far as we are aware, this is the first experimental measurement of the full complex transfer functions for the study of antiphase dynamics in lasers. Knowing the phase and magnitude of the transfer function, information on the contributions of each cavity mode to each of the collective modes can be extracted by determining the residues, as will be discussed below. Typically, the cancellation of the collective modes in the antiphase dynamics about a steady state is not perfect, and by measuring transfer functions the degree to which cancellation occurs can be ascertained, as can the type and extent of the clustering.

The residues are determined by fitting a general transfer function, in the form of a ratio of polynomials, to the data. The order of the polynomials is constrained by counting the number of relevant degrees of freedom. To introduce the terminology, we outline the transfer function analysis and, for concreteness, we do this in the context of rate equations due to Tang, Statz, and deMars (TSdM) [7], modified slightly to include a small pump rate modulation $w = m \sin\omega t$,

$$\tau_f \frac{dn_0}{dt} = w_0 - n_0 - \sum_{i=1}^{N} \gamma_i \left(n_0 - \frac{n_i}{2} \right) I_i + w$$

$$\tau_f \frac{dn_i}{dt} = \gamma_i n_0 I_i - n_i \left(1 + \sum_{j=1}^{N} \gamma_j I_j , \right), \quad i = 1 \ldots N \qquad (1)$$

$$\tau_c \frac{dI_i}{dt} = \left[\gamma_i \left(n_0 - \frac{n_i}{2} \right) - 1 \right] I_i , \quad i = 1 \ldots N.$$

The number of oscillating modes is N, n_0 is the average population inversion and n_j are population inversion components oscillating spatially with the same wavelength as the corresponding laser mode of intensity I_j. The gains of the modes are taken into account through the coefficients γ_j, while τ_f and τ_c represent decay times for the population inversion and the cavity, respectively. Equations (1) assume the inversion density, averaged over a few optical wavelengths, is constant along the axis of the laser mode and the laser medium fills the cavity, but are otherwise appropriate to our Nd:YAG (yttrium aluminum garnet) laser. These assumptions are not strictly valid for our laser, but in the present absence of a better model the TSdM equations are still useful to illustrate how our measurements of transfer functions can discriminate against a model.

Equations (1) can be written in condensed form $d\mathbf{x}/dt = \mathbf{F}(\mathbf{x}) + \mathbf{b}w$, where $\mathbf{x}^T = [n_0, n_1, \ldots, n_N, I_1, \ldots, I_N]$, $\mathbf{b}^T = [1/\tau_f, 0, \ldots, 0, 0, \ldots 0]$. The Jacobian of $\mathbf{F}$ is denoted by $\mathbf{A}$ and is a function of the steady state solution $\mathbf{x}^0$. The sta-

*Electronic address: lstamate@physics.adelaide.edu.au
†Electronic address: mwh@physics.adelaide.edu.au

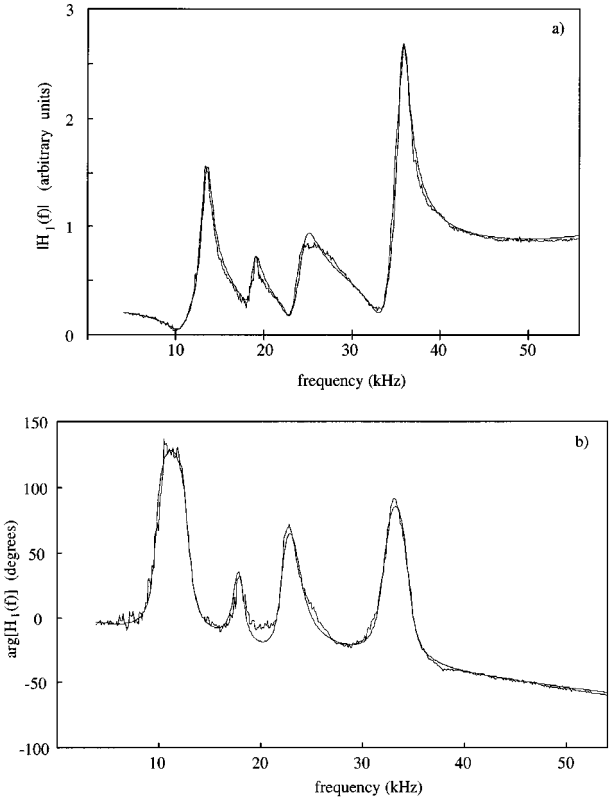

FIG. 1. Transfer function for mode I showing (a) magnitude and (b) phase for the four lowest frequency collective mode resonances. The smooth curves are fits to the data of the generic transfer function, Eq. (2), with $n=11$ poles and $m=9$ zeros.

bility of $\mathbf{x}^0$ can be found in the usual manner by evaluating the eigenvalues λ_i of $\mathbf{A}$. Close to steady state, we have for the deviation from steady state $\tilde{\mathbf{x}}$, $(d\tilde{\mathbf{x}}/dt)=\mathbf{A}\mathbf{x}+\mathbf{b}w$, and by a Laplace transform we obtain the transfer functions [12] $H_i(s)=Y_i(s)/W(s)=\mathbf{c}_i^T(s\mathbf{I}-\mathbf{A})^{-1}\mathbf{b}$, $H_t(s)=Y_t(s)/W(s)=\mathbf{c}_t^T(s\mathbf{I}-\mathbf{A})^{-1}\mathbf{b}$. Here $W(s)$ is the Laplace transform of $w(t)$. The responses Y_i and Y_t for the laser mode i and the total intensity, respectively, are given by $Y_i(s)=\mathbf{c}_i^T\tilde{\mathbf{X}}(s)$ and $Y_t(s)=\mathbf{c}_t^T\tilde{\mathbf{X}}(s)$. The Laplace transform of $\tilde{\mathbf{x}}(t)$ is $\mathbf{X}(s)$ and we use the ''selection vectors'' $\mathbf{c}_i^T=[0,0,\ldots,0,c_{i+N+1}=1,0,\ldots,0]$, $\mathbf{c}_t^T=[0,0,\ldots,0,c_{N+2}=1,1,\ldots,1]$. A transfer function can be expressed either as a ratio of polynomials (pole-zero representation) or as a partial fraction (pole-residue representation) [12]

$$H(s)=\frac{\Pi_{i=1}^{m}(s-z_i)}{\Pi_{j=1}^{n}(s-\lambda_j)}=\frac{r_1}{s-\lambda_1}+\frac{r_2}{s-\lambda_2}+\cdots+\frac{r_n}{s-\lambda_n}. \tag{2}$$

The poles λ_j are the eigenvalues of $\mathbf{A}$, the zeros are z_i and the residues are r_j. We have used the linear stability analysis expressed in this language to analyze the results from our experimental system which we describe below. Interesting insights into the problem can be gained also from the pole-zero representation but we concentrate on the pole-residue representation in this communication.

The laser medium that we used was a Nd:YAG rod cut with one end perpendicular to the rod axis and the other at

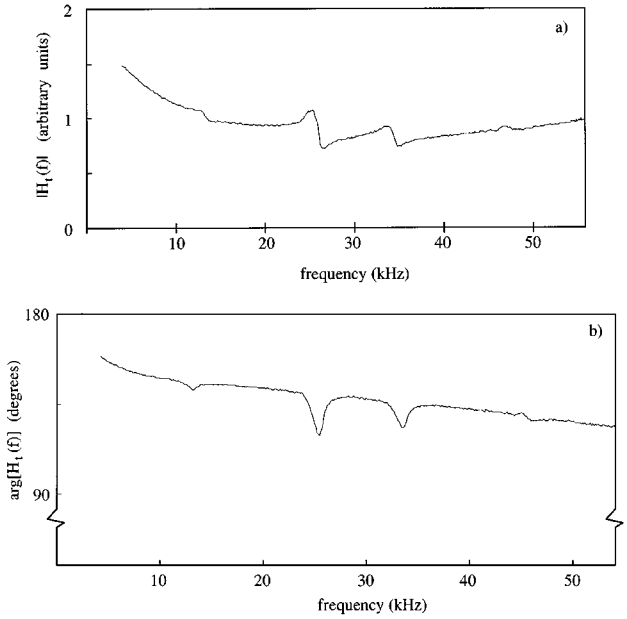

FIG. 2. Transfer function for the total intensity showing (a) magnitude and (b) phase.

Brewster's angle. A high reflection coating on the perpendicularly cut end formed one end mirror of the laser cavity and the output coupler was a partially transmitting mirror ($T=1\%$) mounted on a piezoelectric tube for fine cavity length control. The Brewster cut face served to ensure that all modes were linearly polarized in the same plane. The Nd laser was end pumped by a 40 mW diode laser through the coated end of the rod ($T=65\%$ at 808 nm). The optical path length of the cavity was 24.3 mm corresponding to a longitudinal mode separation of $\delta\nu=6.16$ GHz. Modulation of the pump was achieved with an acousto-optic modulator, which avoided the mode partition noise of the pump laser that can occur if its injection current is modulated. We also had an optical isolator, comprising a polarizer and Fresnel rhomb, between the pump laser and the Nd laser to minimize the destabilizing effects of optical feedback. For comparing the measured transfer functions to the theory, two lifetimes needed to be determined. We measured the cavity lifetime to be $\tau_c=3.56$ ns and took the response time of the medium to be $\tau_f=230$ μs [13].

The output of the Nd laser was split into two beams so that the total intensity and intensity of one mode could be measured simultaneously. With a pump level of about 1.3 times threshold we observed between four and six laser modes, depending on the exact cavity length. The data shown below is for five mode operation. A Fabry-Pérot interferometer was used in one output beam to select individual laser modes and its passband was locked to the relevant laser mode with a lock-in amplifier. The dither that was used in this lock was reduced in amplitude sufficiently that its harmonics were not detectable in the power spectra of the intensity noise for individual modes or total intensity. The fundamental at 3.0 kHz was much lower than the frequencies of interest for the collective mode dynamics. The intensities, total and modal, were measured with low noise photodiode detectors and the outputs of these were directed to a Hewlett Packard HP35670A signal analyzer. For transfer

TABLE I. Measured residues for five mode operation. The columns correspond to the low frequency collective modes and the rows to the laser cavity modes. The magnitudes are in arbitrary units and the phases are in degrees.

Freq	13.3±0.1 kHz		18.7±0.1 kHz		25.6±1.0 kHz		34.6±0.7 kHz		96.1 kHz	
	Mag	Phase	Mag	Phase	Mag	Phase	Mag	Phase	Mag	Phase
Mode I	851.7	71.0	246.3	65.6	908.3	74.1	1739.0	51.0	27 314	−177.2
Mode II	846.8	−103.2	135.1	−117	2267.8	66.0	268.9	−110.6	20 031	−177.2
Mode III	251.9	−98.3	95.5	−130.6	1939.9	−119.8	959.0	57.4	15 692	−174.4
Mode IV	653.3	−108.4	230.0	67.3	1405.0	−119.7	1212.9	−131	15 658	−179.3
Mode V	1285.4	73.9	68.65	5.1	184.0	55.0	1480.8	−129.2	15 561	−174.6

function measurements the analyzer supplies the modulating signal, scanned repetitively in frequency. The results of 1000 frequency scans are averaged to reduce the intrinsic noise of the system. An example of a measured transfer function is shown in Fig. 1 for mode 1 (i.e., the first to oscillate as the pump level is raised past threshold). Four out of a total of five collective mode resonances are visible in this plot. The fifth, which is the normal relaxation oscillation peak, lies at 96.1 kHz. With the HP35670A the complex response can only be measured to 55 kHz; for the resonance at 96.1 kHz we can measure directly only the amplitude squared response $|H(s)|^2$. That we see just five resonances is in agreement with Eqs. (1) from which we predict that the poles, and similarly the residues, are real or arranged in complex conjugate pairs due to the real-valued nature of the matrix A. Shown with the data in Fig. 1 is a fitted transfer function based on Eq. (2). In this fit the linear stability analysis of Eqs. (1) was used to fix the numbers of poles and zeroes [12], and then the resulting ratio of polynomials (i.e., the pole-zero representation) was fitted to the data using a weighted least-squares fit. The curves for the magnitude and phase are fitted simultaneously by the HP35670A analyzer although we found that the fits were better if fine tuned by fixing the positions of the poles and slightly altering the positions of the zeroes that were found by the HP35670A. The measured phase and magnitude of the transfer function for total intensity is plotted in Fig. 2. Here we see, quite clearly, the remaining low frequency resonances and the fact that they have not been completely canceled out by the antiphase dynamics.

By looking at the transfer functions in terms of the partial fraction expansion, we can get a more vivid picture of the antiphase dynamics. In Table I we show the partial fraction decomposition of the measured transfer functions, with the residues expressed as magnitude and angle. These residues were determined by doing the curve fit in terms of the pole-zero representation, as described above, and then converting to the pole-residue representation. The frequencies shown in Table I are those of the poles determined as part of the same fit as that used to obtain the residues. The phases of the residues at 96.1 kHz, the relaxation oscillation frequency, were determined indirectly from fitting to the low frequency data. For comparison we show in Table II residues calculated from the TSdM equations using $w_0=1.308$, which gave the best match between the calculated and measured frequencies of the highest frequency collective mode resonance. The gains γ_i were determined by assuming a Lorentzian profile of width 135 GHz for the gain, normalized to one at the peak using $\Delta\nu=0.246$ GHz for the frequency offset between the first mode to lase and the center of the gain profile. The lifetimes, as given above, were used directly in the calculations. The collective mode frequencies shown in the top row are just the imaginary parts of the calculated poles.

The antiphase dynamics manifests itself as a double clustering of the residue phases which can be seen more easily if they are plotted on a polar diagram as shown in Fig. 3 for the experimentally determined residues of Table I and in Fig. 4 for the calculated residues of Table II. Both calculated and experimental residues show the clusters pointed in opposite directions, though if the magnitude of the residue is small it can sometimes lie outside the clusters. We believe this represents errors in the fit. The apparent rotation of the clusters, both with increasing frequency in the experimental data sets and in the comparison between theory and experiment, is due mostly to frequency dependent phase shifts in the pump modulation.

There are aspects of the data that can serve as a test of theoretical models, as the comparison of Tables I and II shows. First, the calculated and measured pole frequencies do not completely agree. Furthermore, comparing the clustering of calculated and measured residues more closely, we

TABLE II. Theoretical residues for five mode operation. The columns correspond to the low frequency collective modes and the rows to the laser cavity modes. The magnitudes are in arbitrary units and the phases are in degrees.

Freq	13.13 kHz		18.01 kHz		34.24 kHz		37.15 kHz		96.08 kHz	
	Mag	Phase	Mag	Phase	Mag	Phase	Mag	Phase	Mag	Phase
Mode I	0.1283	89.95	0.6740	89.86	0.0226	89.98	1.2468	89.97	22.504	−90.01
Mode II	0.1346	89.93	0.7349	89.84	0.2156	89.97	0.7275	−90.02	17.485	−90.01
Mode III	0.1359	89.92	0.7495	89.84	0.2386	−90.02	0.5373	−90.02	16.645	−90.01
Mode IV	0.3808	89.83	1.9528	−90.08	0.0015	−90.05	0.0253	−90.05	3.4444	−90.02
Mode V	0.8405	−90.06	0.4887	−90.16	0.0008	−90.06	0.0140	−90.05	2.0481	−90.02
Total	0.0608	−89.37	0.2831	−89.65	0.0027	−89.8	0.0573	−89.82	62.127	−90.01

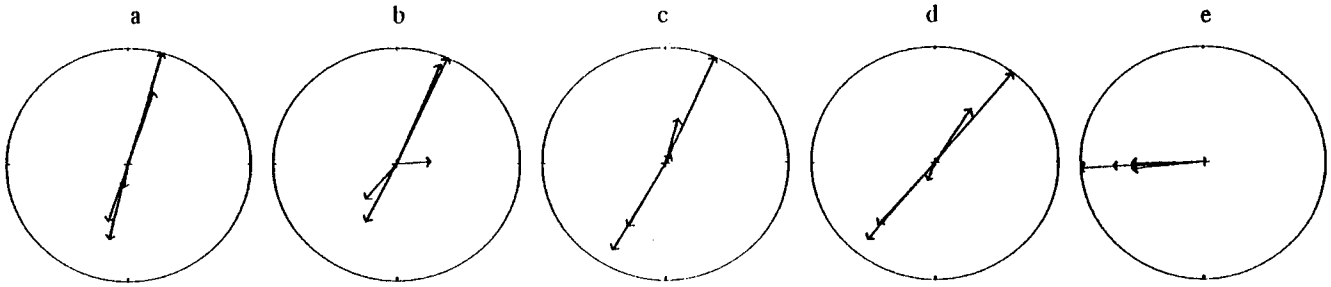

FIG. 3. Polar diagrams of the experimentally determined residues for fitted pole frequencies: (a) 13.3 kHz, (b) 18.7 kHz, (c) 25.6 kHz, (d) 34.6 kHz, (e) 96.1 kHz. In each plot the residues are normalized to that of largest magnitude.

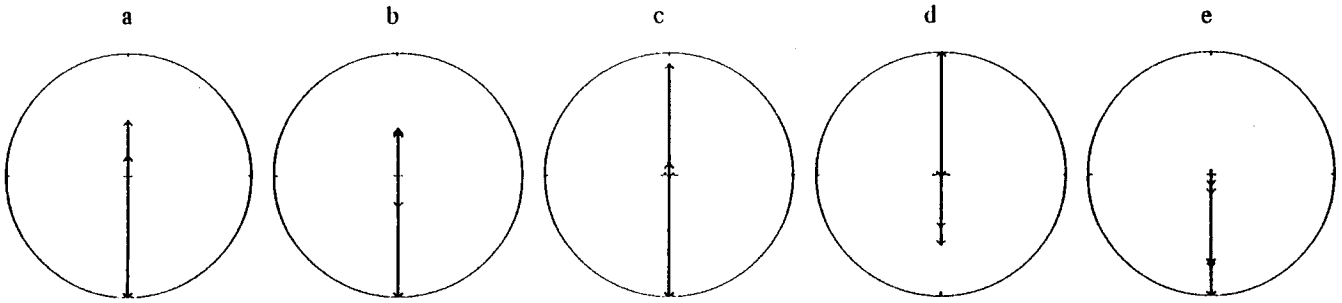

FIG. 4. Polar diagrams of the theoretical complex residues of the poles. The pole frequencies are (a) 13.13 kHz, (b) 18.01 kHz, (c) 34.24 kHz, (d) 37.15 kHz, (3) 96.08 kHz.

can see more discrepancies. In the theory based on Eqs. (1), the phases of the contributions to each resonance from each cavity mode follow a sequence $(+++++-)$, $(++++--)$, $(+++---)$, $(+----)$, $(------)$, as we look at each collective mode in turn (see Table II). A similar ordering of the phases has been previously reported in a numerical analysis of a multimode laser with feedback [14]. Our data do not show this ordering. These discrepancies most likely reflect the known inadequacies of Eqs. (1) when applied to our laser; i.e., concerning the exponential decay of the inversion density and the gain medium not fully occupying the optical resonator. Work to resolve the discrepancies discussed above, by extending the TSdM equations to take into account these factors, is currently in progress. We conclude that the transfer function approach gives much more detailed information and is a more sensitive means of testing models of the dynamics than excitation with broadband noise.

We wish to acknowledge useful discussions and correspondence with K. Corbett and P. Mandel. This work has been supported by the Australian Research Council and the University of Adelaide. Calculations of transfer functions were made using the free software SCILAB developed at INRIA - France.

[1] K. Wiesenfeld, C. Bracikowski, G. James, and R. Roy, Phys. Rev. Lett. **65**, 1749 (1990).
[2] P. Hadley and M. R. Beasley, Appl. Phys. Lett. **50**, 621 (1987).
[3] D. Golomb, D. Hansel, B. Shraiman, and H. Sompolinsky, Phys. Rev. A **45**, 3516 (1992).
[4] J-Y. Wang, P. Mandel, and T. Erneux, Quantum Semiclass. Opt. **7**, 169 (1995).
[5] P. Hadley, M. R. Beasley, and K. Wiesenfeld, Phys. Rev. B **38**, 8712 (1988).
[6] D. E. McCumber, Phys. Rev. **141**, 306 (1966).
[7] C. L. Tang, H. Statz, and G. deMars, J. Appl. Phys. **34**, 2289 (1963).
[8] K. Otsuka, P. Mandel, M. Georgiou, and C. Etrich, Jpn. J. Appl. Phys. **32**, L318 (1993).
[9] P. Mandel, K. Otsuka, J-Y. Wang, and D. Pieroux, Phys. Rev. Lett. **76**, 2694 (1996).
[10] P. Khandokhin, Ya. Khanin, J-C. Celet, D. Dangoisse, and P. Glorieux, Opt. Commun. **123**, 372 (1996).
[11] Yu. D. Golyaev and S. V. Lantratov, Kvant. Elektron. (Moscow) **6**, 2361 (1979) [Sov. J. Quantum Electron. **9**, 1390 (1979)].
[12] F. Blackman, *Introduction to State-variable Analysis* (Macmillan, London, 1977).
[13] W. Koechner, *Solid State Laser Engineering*, 3rd ed. (Springer, Berlin, 1992).
[14] D. Pieroux, P. Mandel, and K. Otsuka, Opt. Commun. **108**, 273 (1994).